Diffusion of chemisorbed oxygen into Pd sub-surfaces and its influence in oxidation catalysis

Sankaranarayanan Nagarajan AND Chinnakonda S Gopinath

Abstract | Oxygen migration to subsurface layers of palladium and its influence in catalytic oxidation has been addressed in this mini review. Oxygen dissolution in palladium is a well-known phenomenon; many researchers observed the presence of surface, subsurface and bulk oxides by different methods on palladium single crystals as well as in powder catalysts. Opinion is divided on deciding the nature of palladium that is responsible for catalytic oxidation reactions. Nonetheless it is tilting towards oxidized palladium, which is likely to be responsible for the oxidation catalytic activity, and increasing numbers of evidences are available. Oxygen covered in the subsurface layers of palladium show extended activity regime to higher temperature and it has been demonstrated by molecular beam methods. CO oxidation studied on Pd surfaces with $CO+O_2$ mixture displays oxidation activity up to 900 K, highlighting a significant increase in CO adsorption capacity on the above surfaces. In this mini review we highlight the oxygen diffusion into Pd-sub surfaces and its characterization by several methods. Further how the subsurface oxygen could influence the electronic structure and hence catalytic activity has been briefly discussed through CO oxidation reactions.

Catalysis Division, National Chemical Laboratory, Dr. Homi Bhabha Road, Pune 411 008, India
cs.gopinath@ncl.res.in

Keywords: Palladium, Oxidation, Heterogeneous Catalysis, Subsurface, Oxygen Diffusion, CO Oxidation, electronic decoupling.

1. Introduction

In the last few decades the number of vehicles all over the world increased to many fold, and as a consequence the air pollution rate also increased drastically, especially in big cities. Simultaneously, governmental regulations also increased all over the world, which stimulated tremendous growth in the research on environmental catalysis; in spite of regulations, overall pollution has increased alarmingly and much needs to be done. The present generation automobile internal combustion (IC) engines are working in the high air to fuel ratio (>14.7) than the stoichiometric value (14.7), to an almost complete combustion of fuel. As a consequence, automotive exhaust contains more oxygen and it is ideal for oxidation, but not for reduction. The active catalyst which is involved in automotive three way catalyst (TWC) are noble metal particles (Pd, Rh, Pt)[1] dispersed on suitable metal oxide supports (Al_2O_3, CeO_2, SiO_2, ZrO_2, La_2O_3 etc). The catalyst is active when the metal particles are in metallic form, and agglomeration to bigger particles as well as oxidation decreases the activity. For many years the classical Pt/Rh catalyst dominated the automotive TWC market; in Europe the Pt/Rh was used in a ratio of about 5:1 and in the US a Pt/Rh ratio of about 10:1 was common.[2] The continuing price rise of noble metals, shrinking Rh supply, and technical improvements in IC engines stimulated an

increasing substitution of Pt and Rh by Pd. One of the first changes in technology was the substitution of Rh by Pd. Pt/Pd catalysts were mainly used in the 1980s. At the beginning of 1990,[2] platinum was replaced by palladium giving the Pt/Pd/Rh (with Pt:Pd:Rh ratios from 1:14:1 to 1:28:1) and finally the Pd/Rh- and Pd-only catalysts. Out of noble metal particles Pd is widely used and replaces the Rh and Pt to a large extent. Although Rh is very active for NO reduction under fuel-rich conditions, this is not the case under net oxidizing conditions, since the excess oxygen inhibits the NO reduction as well as CO oxidation activity of Rh by oxidizing it to Rh_2O_3.[3] Platinum catalysts are reported to be very good for CO oxidation, but the formation of irreversible oxide leads to make platinum to be replaced.[3] Palladium has been suggested as an alternative active element for NO reduction due to significant NO dissociation capacity and its stability at high temperature and under oxidizing conditions, as well as for CO and hydrocarbon oxidation. Palladium based catalysts are more suitable for current automotive catalysts, which doesn't undergo irreversible oxidation even at high air/fuel ratio and the cost is relatively lower than other noble metals. Pd has benefited from the significant advantage called "oxygen storage" capacity.[2] This factor underscores the importance of Pd in TWC converters.

According to United States geological survey, the overall production of palladium was 222 metric tons in 2006 and out of which most of the palladium is utilized in TWC in automobile industry and this underscores the importance of palladium.[2] Present generation IC engines are working at high air/fuel ratio necessitates the need to study the effect of oxygen on Pd-surfaces under various oxygen rich conditions. This is essential due to oxygen diffusion into subsurfaces and the bulk of Pd, depending on the conditions. In this review we focus on the oxygen diffusion into subsurfaces of Pd and its influence in oxidation catalysis. The conditions for oxygen migration to the subsurface of palladium are simple; at temperatures above 500 K and at high oxygen partial pressure, oxygen subsurface diffusion begins, and different surface structure have been observed. Mainly, two dimensional meta stable surface oxide (Pd_5O_4) formation was observed and confirmed by in situ high pressure X-ray photoelectron spectroscopy (XPS), when the partial pressure of oxygen was 10^{-3} mbar on Pd(111) or on prolonged exposure at 10^{-6} mbar between 500 and 600 K.[4,5] Subsurface level is defined as the top few unit cells from the surface and typically it is of the order of 2 nm depth.

Detailed work on CO and O_2 adsorption and CO+O_2 reaction on Pd(111) surfaces has been reported by Engel et al.[6] To understand the molecular level mechanism of CO oxidation and NO reduction on the catalytic converter, well-ordered single crystals of Pd and Rh has been used by various groups.[7–9] Many interesting phenomena were observed, such as the oscillatory nature of CO oxidation with a high O_2:CO ratio. The subsurface migration of oxygen on palladium was observed by many research groups using various surface sensitive techniques; out of which molecular beam technique[8] is the method of our interest and successfully employed to explore the influence of subsurface towards oxidation catalysis.[9]

2. Oxygen diffusion into Pd subsurface — So far

2.1. *General aspects*

There are significant number of studies have been carried out on Pd interaction with oxygen in wide temperature and pressure range which results in the formation of oxide on surface, subsurface, meta stable oxides (Pd_xO_y) and bulk oxide formation.[10–20] On 1969 Sandler et al[16] observed the bulk oxide formation on Pd powder when exposed to oxygen for a long time. The total surface area of palladium powder increased when 400 ML oxygen was deposited. The total surface area of the powder, measured by the BET method with krypton, was 5100 cm^2 for the degassed palladium and 6600 cm^2 after depositing 400 ML of oxygen. Hoffman et al[17] observed that oxygen dissociatively adsorb on Pd above 200 K and it forms p(2×2) Low energy electron diffraction (LEED) pattern at room temperature, which corresponds to 0.25 ML oxygen coverage, with oxygen atom occupying the three fold hollow sites. In general at an oxygen coverage (θ_O) of 0.25 ML on Pd(111) formation of (2×2) structure has been observed by low energy electron diffraction (LEED), and scanning tunneling microscopy (STM) by many groups.[17,19] In the presence of oxygen between 10^{-7} and 6×10^{-5} mbar and the temperature between 573 and 683 K, there is a two dimensional metastable Pd_5O_4 oxide was observed by many research groups.[10,11]

Thirunavukkarasu et al[18] studied NO adsorption and decomposition on Pd(111) through molecular beam technique. It has been observed that at above 475 K, NO dissociation was observed followed by oxygen diffusion into the subsurface. θ_O measured through CO-titration demonstrates a decreasing θ_O above 450 K in spite of significant NO dissociation. Indeed oxygen deposited, due to NO dissociation, disappears from the Pd(111) surfaces $\geq$475 K is also to be noted, which is in agreement with the above. Kinetic oscillation has been observed in the rate of formation of CO_2 from CO+O_2

Figure 1: Thermal desorption spectra of oxygen from Pd(111): (a) after heating to 1273 K and 4000 ML oxygen at 623 K; (b) after exposure to 8000 ML at 973 K and 4000 ML at 623 K; (c) after preparation (b), but desorption to 923 K and cooling to 300 K; (d) after preparation (b) followed by reaction with 300 ML CO at 523 K. (Reproduced with permission from Elsevier)

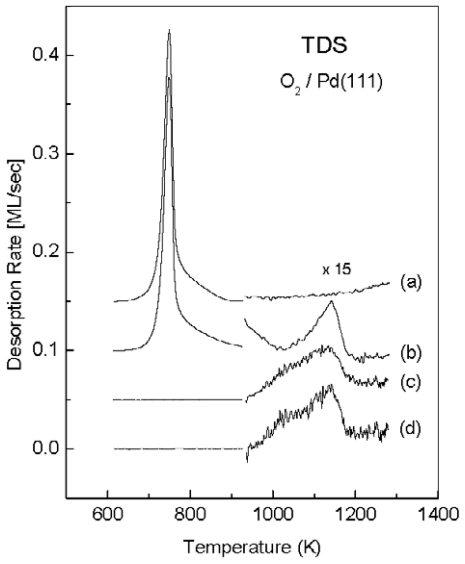

reactions and subsurface diffusion of oxygen on Pd(110) surfaces.[19] It has been demonstrated that the presence of subsurface oxygen decreases the work function beyond $\theta_O = 0.5$ L as oxygen atoms located beneath the topmost layer will be associated with dipole pointing inwards with respect to surface plane. Conrad et al[20] studied the interaction of NO and O_2 on Pd(111) surfaces using LEED, TPD, and UV-photoelectron spectroscopy (UVPES). Titkov et al[10] observed the oxygen diffusion into the subsurface of Pd(110) at $\geq$400 K and the O_2 partial pressure between 2×10^{-8} to 7.5×10^{-2} Torr. Results obtained by temperature programmed desorption (TPD) spectroscopy and XPS indicate that oxygen penetrates into the subsurface layers of palladium ($\geq$ 15–20 Å) and is distributed in a low concentration. Growth and decomposition of the metastable surface Pd_5O_4 oxide on Pd(111)[12] was studied at temperatures between 573 and 683 K and O_2 pressures between 10^{-7} and 6×10^{-5} mbar. Klötzer et al[12] and Leisenberger et al[13] studied the adsorption and desorption of oxygen on Pd(111) surfaces using molecular beam adsorption, low energy electron diffraction (LEED), TPD, and scanning tunneling microscopy (STM), between 300 and 623 K and up to 1 ML using high flux molecular beam of oxygen. It is shown that the formation and decay of p(2×2) surface structure involves a massive rearrangement of surface Pd atoms and change in the surface geometry. Fig. 1 shows the thermal desorption spectra results observed from Pd(111) upon dosage of 4000 ML of oxygen at temperature 623 K.[13] Before that, the Pd(111) was heated to 1273 K. The maximum desorption of chemisorbed oxygen occurred in a single peak at 750 K and there is no oxygen desorption above 900 K; no additional peaks appeared at higher temperatures in Fig. 1a. Fig. 1b was obtained after an oxygen pre-dose of 8000 ML at 973 K, followed by 4000 ML of oxygen at 623 K. This pretreatment was carried out to populate the oxygen into the subsurface levels of palladium, which produces an additional desorption peak at 1142 K. It has been claimed that at least five times higher exposure was necessary to populate the subsurface layers as well as to measure the small thermal desorption feature that occur around 1140 K; it is because of very low defect density in the single crystal, especially with (111) facets. The chemisorbed oxygen can easily be removed thermally by heating up to 923 K (Fig. 1c) or by CO titration at 523 K (Fig. 1d) without markedly affecting the desorption feature at 1142 K. This also indicates that the subsurface oxygen cannot be removed by CO titration. The supply of oxygen to the near surface is relatively easier than oxygen migration to the bulk.

Fig. 2a shows oxygen adsorption from O_2 molecular beam on a clean Pd(111) surface at 900 K.[9] Oxygen flux ($F_{O_2} = 0.33$ ML/s) was used in this experiment. A decrease in O_2 partial pressure at the time of shutter removal ($t = 13$ s) demonstrates a clear O_2 uptake and hence adsorption.[9] It is to be underscored that direct O_2 adsorption observed well above the oxygen desorption range around 750 K, at a significant rate with a measurable adsorption.[9] It is to be underscored that direct O_2 adsorption observed well above the oxygen desorption range around 750 K, at a significant rate with a measurable initial sticking co-efficient (s_o) as well as at later times. It is to be noted that oxygen adsorption continue to occur for a long period, albeit at a lower rate, compared to an initial rate of adsorption; shutter operation has been performed to show the trend of adsorption and desorption throughout the experiment. Desorption occurs exclusively from the chemisorbed oxygen from surfaces only. The intensity of adsorption is always bigger than desorption peak which shows the continuous adsorption even in a desorption regime. This demonstrates the diffusion of adsorbed oxygen into subsurface layers. Subsurface diffusion stops between 500 & 600 s, indicates a saturation of subsurface layers with oxygen. Fig 2b displays the amount of subsurface oxygen coverage $\theta_{O_{Sub}}$ measured from O_2 uptake

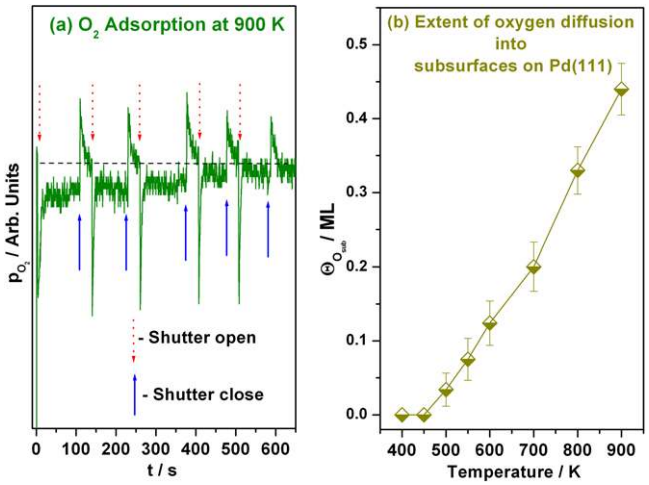

Figure 2: (a) Oxygen adsorption on clean Pd(111) surface kept at 900 K for 1000 sec. The dotted line corresponds to the base pressure level without adsorption or desorption. Note a continuous oxygen adsorption at a slow rate of adsorption for about 500 s before it reaches a state without any further adsorption. Intermittent beam oscillation performed to show the desorption of adsorbed oxygen exclusively from the surface and quickly reaches the background pressure. Upward and downward arrows indicate the open and closed position of the shutter, respectively. (b) Subsurface oxygen coverage ($\theta_{O_{Sub}}$) calculated directly from the oxygen uptake on Pd(111) for 750 s.

at different temperatures. There is no oxygen migration observed to the subsurfaces below 450 K, and it is mild at 500 K. The oxygen migration increases linearly with increase in temperature and about 0.45 ML of oxygen could be accommodated when the temperature is 900 K.

Figure 3 shows the phase diagram of Pd-O system in a wide temperature and pressure regime. Pd(111) structure was slowly converted to PdO with increase in the O_2 partial pressure from 10^{-5} Torr to 1 Torr using high pressure XPS.[4] Surface and subsurface structures formed during the oxidation of Pd(111) has been explored. Initially (2×2) structure forms above 800 K with O_2 partial pressure between 10^{-5} and 10^{-3} Torr. The surface oxide formation with $\sqrt{6}\times\sqrt{6}$ structure has been observed between 650 and 750 K. No "subsurface oxide" is observed during diffusion-controlled reduction. It has been proposed that an epitaxial "subsurface oxide" forms as a metastable intermediate in the bulk oxidation, and that the low activation energy for this process kinetically stabilizes the "subsurface oxide". Bulk PdO forms around 1 Torr between 500–800 K.

2.2. *Structure aspects*

Klötzer et al[12] observed Pd_5O_4 phase using STM, between 573 and 683 K with O_2 pressure between 10^{-7} and 6×10^{-5} mbar. At 683 K the formation of the Pd_5O_4 structure can be divided into two steps: formation of an intermediate phase with oxygen coverage of approx. 0.4 ML followed by growth of the Pd_5O_4 phase. Dissociation of oxygen on the intermediate phase seems to be easier than on the p(2×2)O phase, since oxidation on the intermediate phase proceeds at lower pressure (8.9×10^{-6} mbar, 683 K) than on the (2×2)O phase (3.5×10^{-5} mbar, 683 K). Decay of the Pd_5O_4 oxide layer at 693 K involves rearrangement into the same intermediate $\sqrt{67}\times\sqrt{67}$ R12.2° structure, which finally breaks up into its building blocks, small clusters of uniform size with the unreconstructed metal surface area covered by a p(2×2)O adlayer in between was observed.

Leisenberger et al[13] observed the surface and subsurface oxygen on Pd(111) between 300 and 1000 K using several methods including high-resolution electron energy loss spectroscopy (HREELS). After 40 L dosing of O_2 at two different temperatures (300 and 523 K), LEED patterns were measured. The spots corresponds to 300 K looks sharp and intense half orders, whereas the half-order reflections are weak and diffuse for 523 K, due to decrease in the concentration of oxygen result in subsurface migration. Conrad et al[20] studied by exposing 3 L of O_2 on clean Pd(111) surface at 300 K. The appearance of diffuse half order spots in the LEED pattern which becomes sharper with further increase in the O_2 exposure. After about 8 L exposure a (2×2) and $(\sqrt{3}\times\sqrt{3})$/R30° structures were identified. This structure also is quite resistant to the attack of hydrogen, a reaction which on the other hand very effectively removes adsorbed oxygen. Apparently, this structure originating from the high temperature treatment is not due to adsorbed oxygen but must be associated with a more tightly bound species in the form of a "surface oxide" which is also a precursor to PdO.

Voogt et al[23] studied the oxygen interaction on Pd(111) and polycrystalline palladium with TPD, LEED, XPS, Auger electron spectroscopy (AES), etc. It gave an indication for the formation of surface oxide at higher temperatures (>470 K) and at oxygen partial pressure in the range of 7.5×10^{-7} Torr. XPS shows that almost 0.5 ML PdO on the surface. However, hardly any amount of oxygen could be observed by AES, as its electron beam easily removed adsorbed oxygen, which is more pronounced in Pd(111) than polycrystalline Pd; this suggests that oxygen bounds tightly to the defect sites. Lattice parameters calculated from the complex LEED patterns, neither match with Pd(111) nor PdO, and the structure is more close to speculated PdO(010). The desorption energy calculated from

Figure 3: Phase diagram showing the stability regions of the different palladium oxide structures as a function of oxygen partial pressure and temperature. The points mark the conditions under which XPS data were acquired while increasing the oxygen pressure at fixed temperature (oxidizing conditions). At these points, no change was observed in the spectra over several minutes. The solid line indicates the phase transition of bulk Pd to bulk PdO. The hatched region shows the PdO bulk oxide stability region when the pressure is reduced from 1 Torr at fixed temperature. (Reproduced with permission from ACS).

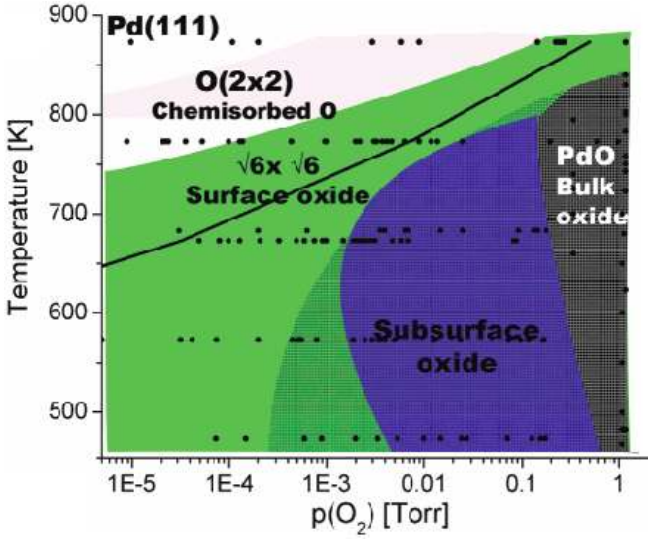

the TPD results is 140 ± 17 kJ/mol and this value is close to the heat of formation of PdO, 112.8 kJ/mo1.

Zheng et al[24] observed the formation of a $(\sqrt{5}\times\sqrt{5})$ R27° reconstruction due to oxygen adsorption on Pd(111) surfaces by STM at >475 K. The images of the $(\sqrt{5}\times\sqrt{5})$ R27° structure are twofold symmetric, consistent with the formation of an epitaxial PdO(001)-like layer. In addition, a (5×5) reconstruction was observed with LEED prior to the $(\sqrt{5}\times\sqrt{5})$ R27° reconstruction. Lundgren et al[25] observed the formation of surface oxide on Pd(111) through STM, and surface X-ray diffraction (SXRD). Structure of surface oxide on Pd(111) was found to be a coplanar Pd_5O_4 overlayer, forming a two-dimensional oxide on the close-packed Pd(111) substrate. Above study revealed that the two-dimensional Pd_5O_4 oxides showing no resemblance to bulk oxides. As per both structure and energetics, the two-dimensional oxide is an intermediate phase between oxygen over layer and a bulk oxide. Oxidation of Pd(110) was observed and the initial $c(2\times4)$ structure which transforms via the formation of anti-phase domain boundaries to a "complex" structure with increasing oxygen partial pressure. Using LEED, high resolution core level spectroscopy and DFT Pd(100)–$(\sqrt{5}\times\sqrt{5})$ R27°-O surface oxide phase was reanalyzed by Todorova et al.[26] A rumpled PdO(001) film suggested by earlier LEED results is incompatible with all three methods employed. Instead, two-dimensional film to consist of a strained PdO(101) layer on top of Pd(100) was suggested.

Lundgren et al[28] observed the oxidation of Pd(100) surfaces in a wide range of oxygen pressure (10^{-6} to 10^3 Torr) and temperature (up to 1000 K) by in situ surface X-ray diffraction (SXRD). Using atomistic thermodynamics calculations, bulk oxide growth was identified even at 675 K. Using SXRD the presence of $(\sqrt{5}\times\sqrt{5})$ R27° surface oxide was confirmed, and bulk oxide film was formed predominantly with PdO(001). The observed diffraction changes significantly as the oxygen pressure and temperature is increased to 10^3 mbar and 675 K respectively, the $(\sqrt{5}\times\sqrt{5})$ R27° surface oxide has completely disappeared from the surface, i.e., the initially formed PdO(101) plane does not continue to grow but instead restructures. It has been shown that there are totally six different states of oxygen on Pd(100), including the first stage of dissociative O_2 chemisorption.[24] A p(2×2) chemisorbed layer was formed up to $\theta_O = 0.25$ ML coverage. Above 0.25 ML both c(2×2) and p(2×2) was observed, followed by high density (2×2) which includes subsurface oxygen, a reconstructed (5×5), and then above 400 K a PdO(001)-like $(\sqrt{5}\times\sqrt{5})$ R27° reconstruction which is further confirmed by STM, and finally bulk PdO. It has been concluded that chemisorbed oxygen is far more reactive toward CO than the PdO(001)-like reconstructed surface which in turn is more reactive than bulk PdO. Markovits et al[29] studied oxygen diffusion on Pd(111) surface from a 3-3 hollow site, the most stable adsorption mode, to a 3–1 hollow site through a bridge site using first-principle quantum mechanics calculations and slab models. The mobility of the surface induces a large restructuring and avoiding the cleavage of the strong (Pd–O) bonds associated with the adsorption was predicted. The surface atoms remain attached to the adsorbate during diffusion was found. An altogether different conclusion derived from above theoretical simulation is that oxygen covered Pd layer slips into the subsurfaces and the metallic Pd layer moves to the surface and this avoids the energetically expensive breaking and making of Pd–O bonds. Although an energetically viable method for oxygen diffusion was suggested by the above calculation,[29]none of the experimental observation indicates the above mechanism.

Zheng et al[24] explored the changes in surface reconstruction due to oxygen adsorption and diffusion into sub surfaces. In order to achieve high oxygen coverage on the sample surface, NO_2 has

been used as a feed molecule; upon NO_2 dissociation oxygen adsorbs on Pd and NO leaves into gas phase. Initial exposure of NO_2 at 500–575 K resulted in a (2×2) LEED pattern as shown in Fig. 4a. Increasing the NO_2 exposure (0.79 L at 575 K) produced new diffraction spots in addition to the spots associated with the (2×2) pattern. As the NO_2 exposure was increased, the intensity of these new spots became stronger, while the (2×2) spots faded, as shown in Fig. 4b–d. The oxygen coverage associated with these changes was 0.25–2.2 ML, and the higher coverage regime advances the TPD peak to 750 K compared 800 K desorption peak at low coverage (0.25 ML). Increasing the NO_2 exposure further into the regime, where the thermal desorption feature associated with bulk PdO decomposition was observed, caused the LEED pattern to fade and the diffuse background to increase.

The LEED patterns in Fig. 4b–d were all obtained at 62 or 63 eV. The spot intensities of these complicated LEED patterns were strongly dependent on energy, and additional spots became visible when the energy was changed. This is illustrated in Fig. 4e, which shows the LEED pattern obtained at 89 eV after an NO_2 dose of 8.1 L, the same exposure as in Fig. 4d. The schematic diagram in Fig. 4f shows the positions of all the observed spots. While the pattern is rather complicated, there are several distinctive features: an inner ring of 18 spots, a second ring of 12 spots, and then groups of three spots. It has been explained with the aid of STM that this pattern is due to three equivalent domains of two different structures.

Figure 4: LEED patterns illustrating structural changes corresponding to the following doses and exposure temperatures: (a) 0.68 L at 500 K, (b) 0.79 L at 575 K, (c) 1.35 L at 575 K, (d) and (e) 8.1 L at 575 K. The sample was rotated between experiments accounting for the different orientations in (a) and (e) compared with (b)–(d). The diffraction spots are shown schematically in (f), where the black solid spots illustrate those due to the Pd(111) substrate. (Reproduced with permission from Elsevier).

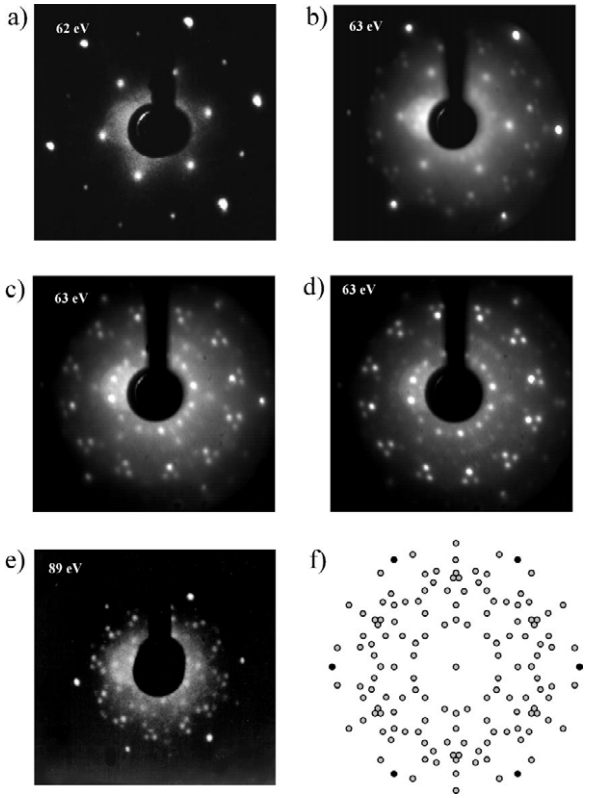

2.3. *Spectroscopy aspects*

Titkov et al[10] studied the O_2 interaction on Pd(110) at 400 K using XPS. O 1s peak was observed at 529.3 eV, and with higher exposure (10^8 Langmuir) the intensity of the peak remained constant which indicates the invariability of chemical state and coverage of oxygen on Pd(110). The XPS analyzer located at 55° with respect to the sample surface provided the analysis depth about 15–20 Å. The presence of oxygen in the subsurfaces of palladium within 15–20 Å was confirmed. Leisenberger et al[13]studied the interaction between oxygen and Pd(111), and subsurface oxygen (B.E. = 529.7 eV) could be distinguished from surface oxygen (B.E. = 529.2 eV) by both XPS and off-specular HREELS by CO titration. Bondzie et al[31] observed the migration of oxygen into Pd(110) subsurfaces and the same has been attributed to be responsible for oscillations in the kinetics of catalytic oxidation of CO. The oxide layer decomposes upon heating in vacuum and results in a much stronger than normal subsurface oxygen desorption event in TPD spectra. Fig. 5 shows HREELS spectra measured in 5° off- specular geometry from (a) Pd(111)-O_I and (b) Pd(111)-O_{II} surfaces before and after a 5L CO dose at room temperature, followed by heating to 423 K.[13] In the specular mode, there is a loss peak was observed at 58.9 meV, mentioned as O_{chem}, is due to chemisorbed oxygen on Pd(111) at 300K. This peak is also present in the HREELS spectrum recorded from the 523 K oxygen dosed Pd surface (lower curve in Fig. 5b). Here, however, there is an additional weaker peak, but clearly observable, loss structure at 40 meV is also observed. It is suggested to be the vibrational modes of oxygen which is present in the subsurface region, and mentioned as O_{sub}. Dosing the Pd(111)-O_{II} surface with 5 L CO and subsequently heating to 423 K removes the O_{chem} peak completely, but leaves the O_{sub} loss peak virtually unaffected (Fig. 5, upper curves). Further, the O_{sub} structure could be removed from the HREEL spectra only after prolonged (about 1 h)

Figure 5: HREELS spectra in 5° off-specular geometry before and after removal of the chemisorbed oxygen by dosing (a) Pd(111)-O_I and (b) Pd(111)-O_{II} surfaces with 5 L of CO followed by a heating to 423 K. (Reproduced with permission from Elsevier).

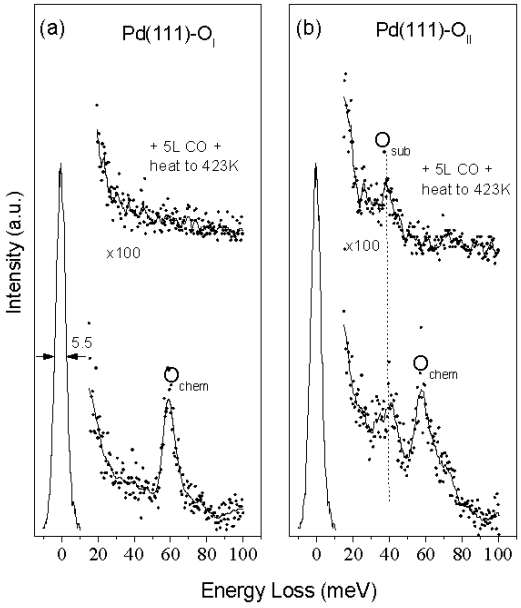

sputtering and annealing treatments (up to 1000 K), again suggesting its subsurface nature. Hence, the loss feature at 40 meV is assigned to vibrations of O located in the subsurface region of the Pd(111) surface. The slow removal of O_{sub} can be further explained by Ar^+ ion sputtering and annealing treatments.

Gabasch et al[32] studied methane oxidation on Pd(111) surfaces at around 10^{-3} Torr O_2 using in-situ XPS. There are three different O 1s peak was observed during heating cycle. An increasing intensity of the O(I) (528.9 eV) and O(II) (529.5 eV) peaks was found between 530 and 650 K, exactly in the temperature range where the catalyst exhibits increasing activity towards the 650 K maximum. Below 500 K, the O(I) and O(II) was found to be less in intensity and a dominant O(III) peak was observed at 530.4 eV. With increasing temperature from 420 to 530 K, O(III) peak decreases, whereas O(I) and O(II) peaks grows in intensity. The O(I) and O(II) peaks at 528.9 and 529.5 eV corresponds to 3-fold and 4-fold coordinated O atoms within Pd_5O_4 surface oxide structures. The Pd_5O_4 surface oxide is characterized by the Pd_{ox1} and Pd_{ox2} peaks at 335.5 and 336.3 eV, which have been attributed to Pd atoms neighboring two and four O atoms, respectively (Figure 6). Importantly the presence of PdO seeds coincides with the pronounced catalytic activity enhancement between ~500 and 650 K. PdO seeds in the Pd_5O_4 ambient represent a particularly active phase for methane oxidation. The Pd_{ox2} component showed a steady growth and reached a maximum at ~550 K, followed by a gradual decrease, whereas the Pd_{ox1} component remained approximately constant up to ~650 K and then started to decrease, indicating the beginning of decomposition of the Pd_5O_4 surface oxide above 650 K. Turnover rate of methane oxidation on PdO seeds is very high, and as soon as this phase appeared the reaction rate increased exponentially at 700 K (see Fig. 7). During the heating cycle, methane conversion starts above 500 K and reaches a maximum at 650 K. Between 650 and 700 K the activity decreases again and finally increases exponentially >700 K. As the temperature increased above 650 K, this most active "PdO seeds + Pd_5O_4" surface state decomposed and the catalytic activity decreased significantly. Above 750 K, the contribution of Pd $3p_{3/2}$ peak increases, which can be attributed to a decreasing total θ_O, and the O(I) component starts to dominate over the O(II) component. Only a single O 1s component at 529.0 eV persists above 850 K. At such high temperatures, this equilibrium shifts toward dissolved oxygen, θ_O becomes small and reaction occurs on the metallic catalyst surface and the reaction rate increases exponentially with temperature.

Gabasch et al[33] observed the formation of 2D oxide phase on Pd(111), which is Pd_5O_4 and supersaturated with O_{ads} layer. The surface was completely covered with 2D oxide between 600 and 655 K and it decomposes completely above 717 K due to diffusion of oxygen into the palladium bulk. During cooling from high temperature and at 2.25×10^{-3} Torr O_2, the oxidized Pd^{2+} species appeared at 788 K; whereas the similar species decomposed at 717 K during heating is to be noted. The surface oxidized states exhibited an inverse hysteresis. The oxidized palladium observed during cooling was assigned to a new oxide phase, probably the $(\sqrt{67}\times\sqrt{67})$ R12.2^o structure. The structural changes and the formation of palladium oxide (Pd_xO_y) are highly dependent on temperature and oxygen pressure.

Kim et al[34] studied the palladium–oxygen interaction using XPS. Both oxygen-chemisorbed palladium atoms (PdO_{ad}) and PdO species has been observed on metal substrates exposed to air at 600 to 900°C. By examining the peak areas of the Pd and the oxygen spectra, the presence of excess oxygen in the form of different species including, hydrated PdO_2, PdO_2, and $Pd(OH)_2$ or $Pd(OH)_4$ were clearly indicated. According to Weissman et al[35], high oxygen exposures of about 10 to 20 L at

Figure 6: Pd $3d_{5/2}$ region of Pd(111) single crystal (1) in the presence of 0.06 mbar O_2 at 573 K (2) and right after switching off O_2. Incident photon energy, $h\nu = 660$ eV. Dashed line: measured data, full line: fits. (Reproduced with permission from Elsevier).

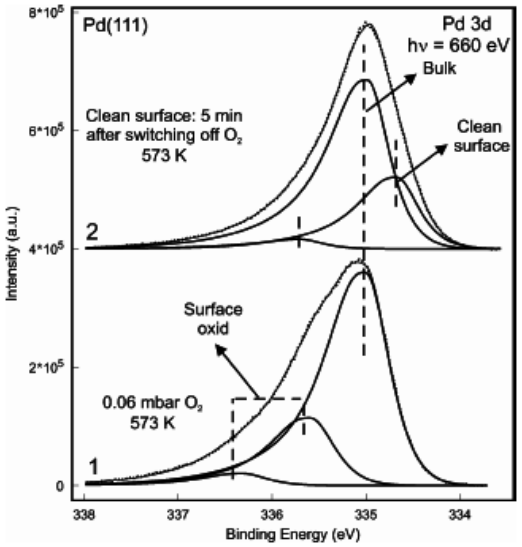

Figure 7: (a) CO_2 and (b) H_2O formation as a function of temperature at a heating–cooling rate of 6.6 K min^{-1}. (Reproduced with permission from ACS).

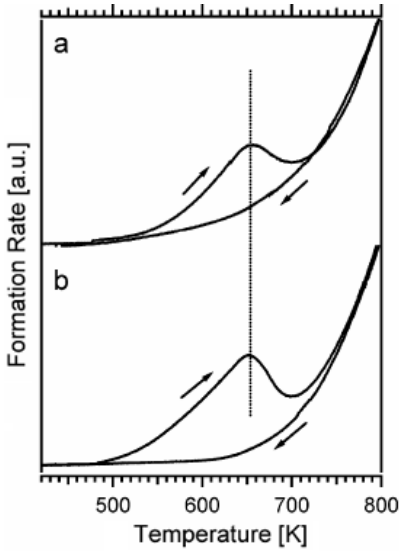

sample temperatures of around 1000 K are the most effective way to populate the subsurface oxygen. Corro et al[36] results showed a direct relation between Pd activity for CH_4 oxidation and the degree of oxidation of Pd species. Nakai et al[37] studied CO oxidation on O-covered Pd(111) surface with fast XPS. The oxygen overlayer is compressed upon CO co-adsorption from a p(2×2) structure into a ($\sqrt{3}\times\sqrt{3}$) R30° structure and then into a p(2×1) structure with increasing CO coverage at 300 K. These three O phases exhibit distinctly different reactivity. p(2×2) phase does not react with CO unless the surface temperature is sufficiently high (>290 K).

Figure 6 describes the importance of in-situ spectroscopy technique to probe the presence of subsurface oxygen. In-situ high pressure XPS has been utilized for Pd(111) at oxygen partial pressure of 0.06 mbar at 573 K.[30] Pd $3d_{5/2}$ core level peak contains contributions from bulk Pd (335.0 eV) and two additional components at B.Es. of 335.6 and 336.3 eV. The Pd $3d_{5/2}$ peak observed at B.E. = 335.6 eV was attributed to adsorbed oxygen, and the 336.3 eV peak was attributed to a new surface oxide phase Pd_5O_4.[30] On turning-off O_2 supply, all the high B.E. features, >335 eV, disappears demonstrating the highly meta stable nature of surface oxide species. This metastable oxide phase is considered to be the precursor state before the oxygen diffusion into subsurface begins. The above point illustrates that, in-situ techniques are more important to measure the observation of metastable oxide formation on any surface.

2.4. *Methane oxidation aspects on Pd surfaces*

There are number of oxidation catalysts has been reported based on Pd metal and being used for various reactions. Pd particles, especially nano palladium supported on Al_2O_3, act as good catalyst for methane oxidation. Some of the important features observed by several researchers about the status of Pd are discussed in this section. Hicks et al[38] studied the effect of catalyst structure on methane oxidation over palladium on alumina. It has been observed that Pd particles are oxidized, and the extent of oxidation increases further with decrease in the particle size and an increasing number of crystal defects. All the oxides present on the surface is directly involved in methane oxidation. The reaction rate depends on the structure of oxidized palladium surfaces. Interestingly it has been concluded that the palladium oxide dispersed over the alumina is much less active than the alumina dispersed over the surface of the palladium crystallites. Farrauto et al[39] also observed that methane oxidation readily occurs when the catalysts contains PdO. Moreover, it has been suggested that palladium metal is inactive towards methane oxidation, and PdO is the active phase of the catalyst. It has been observed that the decomposition or reduction of PdO/Al_2O_3 to Pd/Al_2O_3 results in a decrease in the activity of palladium for methane oxidation. Lyubovsky et al[40] studied methane

oxidation on Pd supported on α-Al_2O_3 and argued that above 760°C the metallic Pd state of the catalyst is formed and upon cooling it transforms into the more active PdO state. This is supported by recent 'PdO seeds' observation by Schlögl et al.[30,32–33]

Adsorption and decomposition of methanol on clean and oxygen covered Pd(111) surfaces using static secondary ion mass spectrometry (SSIMS) and XPS.[41] SSIMS results displayed a variety of ions that includes Pd_mO^+ (m = 1, 2), $PdOCH_3^+$, $PdCH_3^+$; and Pd_nCO^+ (n = 1–3) Similarly, Burch et al[42] also conclude that metallic palladium is not active for methane oxidation. Further, chemisorbed oxygen is less active than oxidized palladium surfaces, and it has been found that there is no loss of activity when the palladium is fully oxidized. Dynamics of oxidation of Pd upon methane oxidation has been observed by Su et al.[21] Initial oxide formed upon oxygen uptake is amorphous, and subsequently transforms to crystalline PdO. Oxygen is dissociatively adsorbed on the surface of the Pd particles forming a monolayer of adsorbed oxygen atoms and oxidation of the bulk Pd begins above 473 K. The activity of Pd is negligible unless it is oxidized.

2.5. *CO oxidation on Pd-surfaces containing sub-surface oxygen*

Thirunavukkarasu et al[18] carried out CO titration on NO dissociated at different temperature on Pd(111) surface and decrease in the CO_2 production was observed when the NO dissociation temperature increased from 450 to 525 K, mostly due to subsurface diffusion of oxygen above 500 K. Bondzie et al[22] investigated the kinetics of oxide formation and its reduction by CO on Pd(110) surfaces. The rate of oxide reduction measured was found to be $r = 2.38\times10^5 \quad p_{CO}\ e^{0.37/RT}$ at 350 K (1.34 ML/s) and at 400 K (14.1 ML/s) agree approximately with the value determined by Ertl et al $r = 9\times10^8\ e^{-14/RT}$at 350 K (1.6 ML/s) and at 400 K (19.9 ML/s) and others[6,27] for chemisorbed oxygen, indicating that the oxide species is weakly bound or unstable. Figure 7 displays the rate of products formation from methane oxidation on Pd(111) surfaces using in-situ XPS during heating and cooling cycle at a pressure of 0.33 mbar reaction mixture.[32] During heating, the rate of production of CO_2 and H_2O was exhibited an activity maximum at 650 K, whereas no activity maximum was found during the subsequent cooling ramp. This kinetic hysterics was assigned to the spectroscopically observed difference in the surface oxidation state. During heating, the reaction rate approached a maximum at 650 K in the stability range of bulk PdO seeds among the otherwise Pd_5O_4 2D oxide covered surface. On the other hand, no PdO seeds were formed during cooling, most likely due to kinetic limitations of PdO nucleation on a passivating surface oxide layer containing less oxygen than Pd_5O_4.

Roy et al[43] used solution combustion method to synthesis $Ti_{1-x}Pd_xO_{2-\delta}$ for the first time, a new photo catalyst for CO oxidation, NO reduction and C_xH_y oxidation purpose. The photo catalytic activity was investigated by varying Pd content and 1 atom% of Pd ion is found to exhibit high activity. High rates of photo oxidation of CO with O_2 over $Ti_{1-x}Pd_xO_{2-\delta}$ are observed at room temperature. It was shown that enhanced CO oxidation at Pd^{2+} ion site and O_2 or NO photo dissociation at oxide ion vacancy is responsible for the enhanced catalytic activity. Baidya et al[44] synthesized $Ce_{1-x}Sn_xO_2$ ($x = 0.1$–0.5) solid solution and its Pd substituted analogue by a single step solution combustion method. Oxygen storage capacity of $Ce_{1-x}Sn_xO_2$ was found to be much higher than that of $Ce_{1-x}Zr_xO_2$ due to accessible Ce^{4+}/Ce^{3+} and Sn^{4+}/Sn^{2+} redox couples between 200 and 400 °C. Pd^{2+} ions in $Ce_{0.78}Sn_{0.2}Pd_{0.02}O_{2-\delta}$ are highly ionic, and the lattice oxygen of this catalyst is highly labile, leading to low temperature CO to CO_2 conversion. The rate of CO oxidation was 2 μmol/g sat 50°C. Thus, Pd^{2+} ion substituted $Ce_{1-x}Sn_xO_2$ was suggested to be a superior catalyst compared to Pd^{2+} ions in CeO_2, $Ce_{1-x}Zr_xO_2$, and $Ce_{1-x}Ti_xO_2$ for low temperature exhaust applications due to the involvement of the Sn^{2+}/Sn^{4+} redox couple along with Pd^{2+}/Pd^0 and Ce^{4+}/Ce^{3+} couples.

Oxygen storage with nano palladium clusters on ordered Fe_3O_4 film has been reported.[45] Pd particle size has been varied between 2 to 100 nm. For low metal loading and small particles, oxidation is highly efficient, but the total oxygen-storage capacity is limited by the small amount of Pd available per catalyst surface area. Formation of Pd oxide becomes kinetically hindered for high metal loading and large particles. The maximum oxygen uptake is observed at intermediate Pd loading at a particle size 7 nm. Here, the particles are large enough to allow substantial amounts of interface oxide to be formed (between Pd particles and support) but are yet small enough to avoid strong kinetic hindrance to oxide formation. It is to be noted that the oxide formed is at the metal-support interface and there is no metal oxide on the surface is reported. Very recently CO-oxidation on Pd(111) surfaces has been reinvestigated and the effect of sub-surface oxygen on CO-oxidation was addressed in detail, by molecular beam techniques.[9] CO oxidation has been measured with various ratios of CO and

Figure 8: Temporal evolution of the beam compositions of $CO:O_2$ [(a) 7:1, (b) 4:1, (c) 2:1, (d) 1:2, (e) 1:4, (f) 1:10] during the transient state of the $CO+O_2$ reaction at 800 K on Pd(111). Transient kinetics of CO, O_2 and CO_2 on fig 8 (c) is encircled to show the delay in CO_{ads} and CO_2 production. The steady state reached fast with oxygen-rich beams is to be noted.

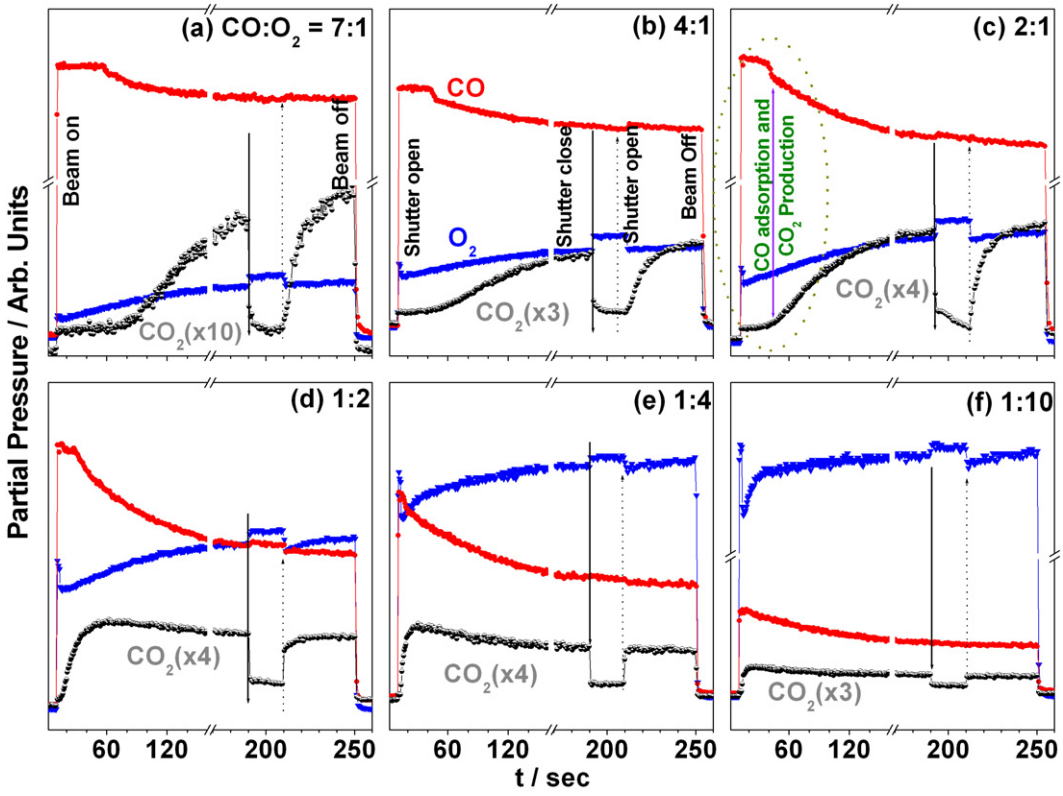

O_2 to demonstrate that the initial oxygen (from the $CO+O_2$ beam) adsorbed on Pd(111) surface diffuses into the subsurface levels of palladium, and after attaining the threshold subsurface coverage the actual oxidation reaction begins on the surface. Indeed no significant CO adsorption was observed, especially at high temperatures (>600 K), till the threshold ($\theta_{O_{Sub}}$) occurs. The amount of oxygen that is present in the subsurface levels of Pd(111) surfaces increase with increase in temperature up to a threshold value under UHV conditions; however no further oxygen uptake occurs above the threshold coverage ($\theta_{O_{Sub}}$). In this process, the top few layer of metallic Pd is converted to a mildly oxidized form ($Pd^{\delta+}$), and hence the metallic bulk Pd is decoupled from the surface due to this process.

Figure 8 shows the beam composition dependence of $CO + O_2$ reactions on clean Pd(111) surfaces at 800 K.[9] The $CO:O_2$ composition has been varied from CO rich (7:1) to oxygen rich (1:10). There is a dip observed in the partial pressure of O_2 observed immediately after shutter removal for all $CO:O_2$ compositions at $t = 13$ s, which indicates that the nature of the clean metal surface at the beginning of the reaction goes towards O-covered Pd(111). Notably, simultaneous CO adsorption (and CO_2 production) was not observed with CO-rich beams. CO adsorption and CO_2 production begins after a delay time (Γ), and this delay depends on the reaction temperature and $CO:O_2$ composition. Γ decreases systematically from 77 s for a CO rich 7:1 composition at 800 K to no delay (0 s) for oxygen-rich compositions above 1:4 (Fig 9a). The above decrease in Γ is due to an increase in oxygen flux (F_{O_2}) with increasing oxygen content in the beam, and hence, the rate of oxygen supply increases, which results in faster diffusion of oxygen to the sub surfaces. CO adsorption begins only on Pd(111) surfaces that contain oxygen atoms on the surface as well as sub surfaces. This demonstrates that the oxygen atoms deposited during the initial delay time at high temperatures diffuses almost exclusively to the subsurfaces, and hence, there is no effective reaction, even though high F_{CO} was available from the beam. With a sufficient amount of oxygen available in the sub surfaces, the electronic

Figure 9: (a) Time delay in the beginning of CO adsorption as well as CO_2 production on Pd(111) surfaces is plotted for different temperatures and $CO:O_2$ ratios. Reactive sticking coefficient of (b) CO and (c) O_2 measured under steady-state reaction conditions for all $CO:O_2$ compositions between 500 and 800 K on Pd(111) surfaces.

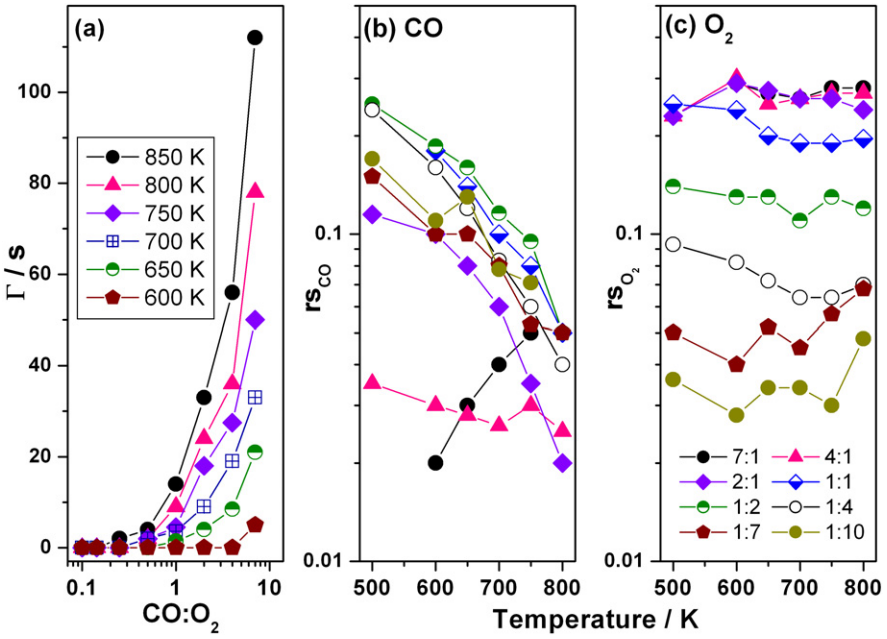

nature of palladium changes from metallic (Pd^0) to mildly oxidized ($Pd^{\delta+}$), and δ depends on the amount of oxygen in the subsurfaces. Some amount of metastable Pd_xO_y formation on the surface and immediate sub surfaces cannot be ruled out.[9]

Figure 9a shows a plot between the time delay (Γ) in CO_{ads} and/or CO_2 production in seconds and the $CO:O_2$ beam ratio.[9] CO-rich beams show a relatively large delay in CO_2 production among the beam compositions. The above time delay decreases with decreasing reaction temperature and with increasing O_2 content in the beam. A systematic decrease in Γ with increasing oxygen content suggests an enhanced rate of oxygen diffusion into the sub surfaces at high F_{O_2}. Especially with decreasing F_{CO}, attaining the threshold $\theta_{O_{Sub}}$ becomes faster. Expectedly, oxygen-lean compositions take a longer time to attain $\theta_{O_{Sub}}$. The time delay also increases linearly as a function of the $CO:O_2$ composition, especially at high temperature, say >700 K, due to decreasing reactive sticking coefficient (rs_{O_2}). This may be attributed to competition between oxygen diffusion into the subsurface and oxygen desorption, since oxygen desorption begins around 750 K. Fig 9b and c show the plots for reactive sticking coefficient values observed in the steady state for CO (rs_{CO}) and O_2(rs_{O_2}) from $CO+O_2$ mixed molecular beams for different $CO:O_2$ ratios and temperatures. With CO-rich beams the (rs_{CO}) varies between 0.02 and 0.25 in the steady state depending on the beam composition and temperature. CO-rich beam compositions show low (rs_{CO}) values around 0.03; however, with increasing oxygen content in the beam and with decreasing temperature to 500 K, the (rs_{CO}) value increases to 0.25. It is to be emphasized here that clean Pd(111) surfaces show hardly any measurable CO sticking coefficient above 525 K,[6,9] highlighting a dramatic change in the electronic nature of Pd-surface that contains significant oxygen coverage in sub-surfaces. It is to be noted that the CO-rich (7:1) beam shows a decreasing (rs_{CO}) value with decreasing temperature and is in good agreement with reported values.

The (rs_{O_2}) values plotted in Figure 9c display a strikingly contrast to that of rs_{CO} pattern in Fig.9b. Irrespective of reaction temperature, rs_{O_2} shows a similar value and hardly there is any variation for a given $CO:O_2$ composition; and this rs_{O_2} value increases with increasing CO content in the beam. Especially rs_{O_2} for CO-rich beams shows a value between 0.2 and 0.3, indicating a significantly large adsorption of oxygen onto Pd(111) surfaces under SS conditions between 500 and 800 K. This is attributed to the large number of vacant sites available in the above temperature range, since the

Figure 10: Steady-state rate of the CO+O_2 reaction as a function of temperature for various beam compositions. The stoichiometric ratio (2:1 to 1:2) shows a maximum steady-state rate in all temperature ranges and the dotted line shows the CO_2 production trend from 500 to 700 K for CO+O_2 (0.75:1) reported by Ertl et al (J. Chem. Phys. **1978**, 69, 1267–1281). Considerable higher rate is observed from the Pd(111) surfaces that contains subsurface oxygen compared to clean Pd(111).

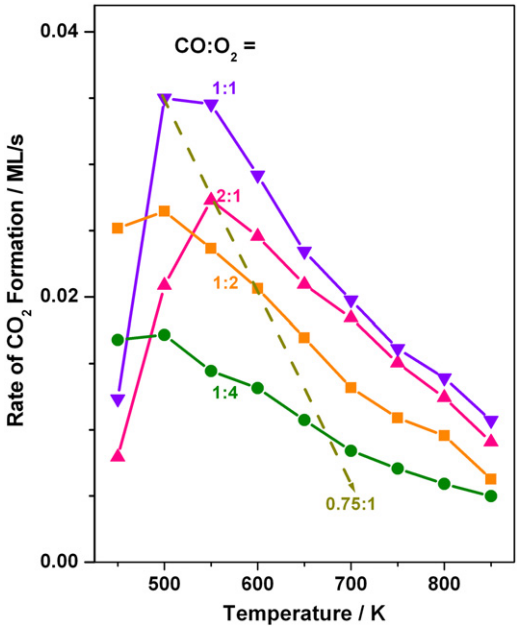

CO desorption rate is very high. Nonetheless, with O_2-rich beams this cannot be true, since there is significant to high θ_O due to high F_{O_2} values. Hence, a relatively steep decrease in rs_{O_2} is observed with increasing O_2 content in the CO+O_2 beams. High rs_{O_2} values observed with CO-rich beams in the SS are comparable to those of sO_2^0 value reported for clean Pd(111) surfaces and underscore the high adsorption probability,[6,9] even at high temperatures (>600 K). Similar rs_{O_2} values observed for a given beam composition also support the onset of the CO oxidation reaction at high temperatures only after $\theta_{O_{Sub}}$ is attained. If oxygen diffusion to sub surfaces continues beyond $\theta_{O_{Sub}}$, rs_{O_2} is also expected to increase with increasing temperature, which is not observed.[9] Hence, it is clear that $\theta_{O_{Sub}}$ does not change with the oxygen content in the reaction mixture, but only with temperature, which supports the view of electronic decoupling of the surface layers from bulk Pd.[9]

Figure 10 provides the steady state CO_2 production rate against the reaction temperature as well as beam composition.[9] A few interesting points are worth highlighting from this figure: (1) There is an optimum reaction temperature range, between 500 and 550 K, where a maximum in rate is reached for CO:O_2 beam compositions that are closer to the stoichiometric composition (CO:O_2). (2) The above optimum temperature range broadens to a wider temperature range, somewhere between 450 and 750 K, for CO:O_2 beam compositions that are either CO-rich or O_2-rich compositions. (3) It is interesting to note the lower rates for 1:4 compositions between 600 and 800 K, suggesting the low-flux reactant component decides the overall rate of the reaction. Alternatively, it may be viewed that the reaction rate becomes less sensitive to the beam composition at high temperatures. All of the above observations demonstrate that the reaction rate is effectively controlled by both the surface temperature and the beam composition below 600 K. Indeed the dotted line in Fig. 10 corresponds to the rate of CO_2 production from 500 to 700 K observed by Ertl et al[6] for CO:O_2 = 0.75:1. The rate maxima observed for stoichiometric CO:O_2 beam (1:1) and (0.75:1) compositions is at 500 K and the rate observed at high temperatures is normalized to the above maxima. Rate decreases with increasing temperature in both cases. The rate approaches significantly to lower value on clean Pd(111) surfaces even at 700 K,[6] whereas significantly high CO_2 production is observed in our results even at 800 K.[9] The enhanced CO adsorption is solely responsible for CO_2 production. In our case the presence of oxygen in near or sub surface levels of palladium makes CO oxidation up to 900 K.

3. Reaction mechanism

Figure 11 describes a schematic representation of CO and O_2 adsorption on Pd(111) surfaces.[9,46] Fig. 11a shows the reactant molecule (CO and O_2) approach the clean Pd(111) surface, Fig. 11b shows the clear adsorption of O_2, especially from CO-rich beam compositions at temperatures higher than 550 K, followed by dissociation into oxygen atoms, whereas CO shows no net adsorption. Fig. 11b–c shows oxygen atom diffuses into the subsurface levels of Pd(111), which changes the surface electronic property of Pd(111), and the palladium acquires a mild positive charge due to the presence oxygen in the subsurface levels; Fig. 11d shows the CO adsorption on $Pd^{\delta+}$(111) surfaces and only after oxygen diffusion into subsurfaces. The product CO_2 formed upon the reaction between adsorbed CO and O in Fig. 11e, and the CO_2 desorption from the mildly oxidized Pd(111) surface is displayed in Fig. 11e and Fig. 11f respectively. Above illustration sketches the various steps involved in CO oxidation on Pd surfaces.

The kinetic data discussed briefly gives some new information on reaction mechanism of CO oxidation with O_2 on Pd(111) surfaces, which is

Figure 11: Schematic representation of oxygen diffusion into the subsurface, partially oxidized palladium and CO oxidation and CO_2 desorption.

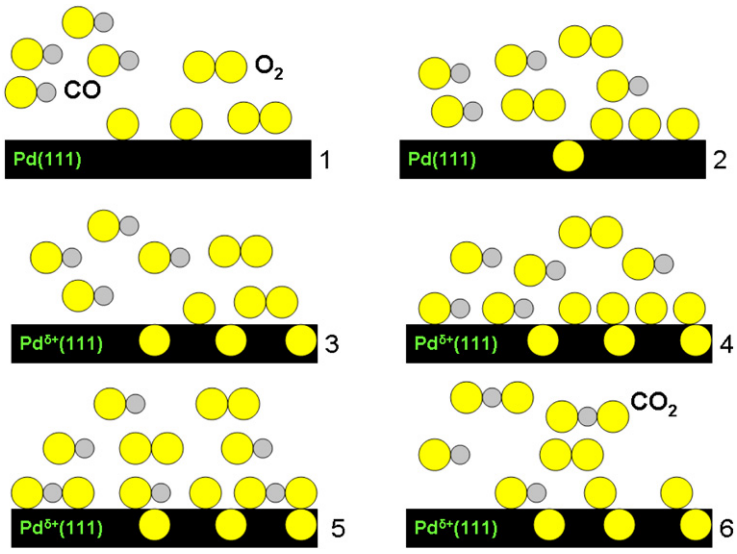

diffusion of oxygen into the subsurface of palladium above 500 K and the associated changes in surface electronic nature. CO rich beams show a delay in CO adsorption and CO_2 production in transient kinetics; however unambiguous O_2 adsorption from all beam composition has been observed without any delay. The above O_2 adsorption involves in the population of subsurface levels of palladium to a threshold coverage, and the subsurface coverage ($\theta_{O_{Sub}}$) increases with increase in the reaction temperature. Elementary steps involved in the reaction mechanism are shown below. Apart from the usual steps, a new stage is included on oxygen diffusion into subsurfaces. In the first step O_2 molecule adsorbed on Pd surfaces dissociates into atomic oxygen to two adjacent sites at >200 K. Diffusion of oxygen into the subsurface levels of palladium begins at 500 K, which is increasing further with increase in temperature (2). About 0.45 ML of oxygen migration could be achieved at 900 K.[9] The migrated oxygen atoms changes the electronic nature of surface Pd atoms to partially oxidized Pd ($Pd^{\delta+}$), high temperature CO adsorption occurs (3) on partially oxidized Pd results in CO_2 formation and subsequent desorption (4).

$$O_{2gas} + 2* \xrightarrow{k_1} 2O_{ads} \quad (1)$$

$$O_{ads} \xrightarrow{k_2, \geq 500K} O_{sub} \quad (2)$$

$$CO_{gas} + * \xrightarrow{K_3} CO_{ads} \quad (3)$$

$$CO_{ads} + O_{ads} \xrightarrow{K_4} CO_{2_{ads}} \xrightarrow{fast} CO_2 \quad (4)$$

It is to be noted that CO adsorption decreases exponentially >500 K due to increasing rate of CO-desorption. Therefore, the CO_2 production rate at high temperatures is dependent on the CO adsorption capacity, which is induced by the changes in electronic nature of surfaces, particularly, subsurface oxygen coverage, and hence, significant CO-oxidation occur and sustained. It is likely that Pd surfaces lose a considerable amount of the surface electron cloud at high temperatures. Hence, the surface electronic nature is significantly different at high temperature compared to low temperatures (<500 K) for Pd surfaces and consequently CO ($^{\delta+}$C–O) adsorption is diminished. At the same time, an adsorbed O atom to diffuse into the subsurface region was observed. However, the presence of oxygen in the subsurface levels recovers electron density from the bulk at high temperatures and makes the top atomic layers mildly oxidized. This makes CO adsorption possible at higher temperatures, and production of CO_2 molecules begins.[9] A simplified jellium model[47] has been invoked to explain the above changes.[9]

4. Carbon subsurface diffusion and its impact in catalysis

Very similar to oxygen diffusion into Pd subsurfaces, carbon diffusion and dissolution into subsurfaces and bulk, respectively has been reported.[48–51] Some of the important aspects of the above has been presented here. It is worthwhile to note about diffusion of carbon into the subsurface of Pd and its influence in catalysis. Bowker et al[48] observed the diffusion of carbon in the subsurfaces of Pd(110) with ethene as a source reactant. Initially ethene adsorbs between 130 and 800 K with high initial sticking probability (s_0) from 0.8 (at 130 K) to 0.35 (at 800 K). Above 450 K, ethene adsorption is continuous with hydrogen evolution and carbon deposition into the surface and the presence of carbon is found to be in top few layers. Above 450 K, carbon diffuses into the subsurface levels of Pd. Steady state ethene decomposition along with diffusion of C into subsurfaces with continuous H_2 desorption was observed >450 K . The presence of carbon is identified by XPS, and it can be removed by reaction with oxygen. LEED or STM patterns doesn't show any well-ordered structures, however, some evidence for a c(2×2) structure has been observed. Very recently, clean-off of carbon by gas-phase oxygen has been addressed.[48] It is important to mention the conclusion that Pd(110) single crystal can be converted completely to PdC with molecular beam reaction setup, and it would take 3×10^5 hours or 30 years with the ethene flux of 1.5 $\times10^{17}$ molecules m^{-2} s^{-1}. If the same experiment

could be at atmospheric pressure with same rate of diffusion, it would take 1 sec to form PdC. If the Pd is on high surface area support, with 3 nm hemispherical Pd particles (~200 surface atoms) it would take about 15 min to form PdC under molecular beam conditions.[48]

Very similar to the above report, Schlögl et al[49] observed carbon diffusion in Pd(111) during ethene oxidation. Ethene oxidation was carried out both on clean metal and carbon dissolved Pd(111). Carbon diffusion starts at 480 K which leads to subsurfaces modification and the dissolved carbon in Pd(111) appears at 284.5 eV in XPS at ~500 K. The electronically altered carbon containing Pd(111) preferentially catalyzes CO formation. A reduced lifetime of CO on the electronically altered surface may specifically favors CO desorption and this might be the reason for selective formation of CO on Pd_xC_y. Goodman et al[50] found the formation of PdC in the synthesis of vinyl acetate using Pd/SiO_2 with two different particle sizes as well as with mixed metals Pd-Au/SiO_2. The smaller Pd particles showed greater resistance to the formation of PdC_x. The combination of Au with Pd is apparently very effective in preventing PdC_x formation in Pd-based catalysts for vinyl acetate synthesis.

Schlögl et al[51] observed that alkynes can be selectively hydrogenated to alkenes on carbon incorporated Pd catalysts in the near surface of palladium. Carbon from the feed molecules (ethyne, propyne and 1-pentyne) has been involved in the diffusion to the subsurfaces and the diffused carbon occupies the interstitial lattice sites. Better selectivity with controlled hydrogenation to alkenes was observed if more carbon is present in the subsurface levels of Pd. However, the same reaction on clean Pd surfaces leads to total hydrogenation.

5. Conclusions

The presence of subsurface oxygen and its influence in overall kinetics, particularly transient-state kinetics has been addressed here. Oxygen diffusion into subsurfaces of palladium has been demonstrated by various techniques like thermal desorption spectroscopy, high resolution electron energy loss spectroscopy, photoemission spectroscopy, low energy electron diffraction, and molecular beam. The formation of ordered surface structures has been confirmed in LEED and STM at different conditions. $\theta_{O_{Sub}}$ increases up to 0.42 ML on Pd(111) surfaces at 900 K with pure O_2 beam. The presence of subsurface oxygen changes the electronic state of Pd surfaces toward a mildly oxidized ($Pd^{\delta+}$) state, and likely an electronic decoupling occurs between the bulk and top few surface atomic layers, of the order of 2 nm. Subsurface modification opens up an area, where extended activity to high temperatures and different selectivity has been observed. It is expected that more work in this area would lead to better catalytic activity with minor modifications in the sub-surfaces and surfaces of existing catalysts.

Acknowledgements

We thank Prof. S. Surnev, Univ. Graz, Austria for readily supplying two original figures. CSG thanks Prof. Mike Bokwer for useful discussions. SN thanks CSIR, New Delhi for research fellowship.

Received 18 June 2010.

References

1. (a) Shelef, M.; Graham, G. W. "Why Rhodium in Automotive Three-Way Catalysts?" *Catal. Rev. Sci. Eng.* **1994**, 36, 433–457. (b) Kreuzer, T.; Lox, S. E.; Lindner, D.; Leyrer, J. "Advanced exhaust gas after treatment systems for gasoline and diesel fuelled vehicles" *Catal. Today* , **1996**, 29, 17–27. (c) Taylor, K. C. "Nitric Oxide Catalysis in Automotive Exhaust Systems" *Catal. Rev. Sci. Eng.* **1993**, 35, 457–481. (d) Shelef, M. "Selective Catalytic Reduction of NO_x with N-free Reductants" *Chem. Rev.* **1995**, 95, 209–225. (e) Belton, D. N.; Taylor, K. C. "Automobile exhaust emission control by catalysts" *Curr. Opin. Solid State Mater. Sci.* **1999**, 4, 97–102. (f) Shelef, M.; McCabe, R.W. "Twenty-five years after introduction of automotive catalysts: what next?" *Catalysis Today,* **2000**, 62, 35–50.
2. (a) Reinhard, B. *Palladium Emissions in the Environment, Automotive Catalysts, Springer Berlin Heidelberg* (Book Chapter). (b) Kielhorn, J.; Melber, C.; Keller, D.; Mangelsdorf, I. *Int. J. Hyg. Environ. Health* **2002**, 205, 417–432.
3. (a) Gopinath, C. S.; Zaera, F., "A Molecular Beam Study of the Kinetics of the Catalytic Reduction of NO by CO on Rh(111) Single-Crystal Surfaces" *J. Catal.* **1999**, 186 **,** 387–404. (b) Tagliaferri, S.; Köppel, R. A.; Baiker, A. "Comparative behaviour of standard Pt/Rh and of newly developed Pd-only and Pd/Rh three-way catalysts under dynamic operation of hybrid vehicles" *Stud. Surf. Sci. Catal.* **1998**, 116, 61–71. (c) Johánek, V.; Schauermann, S.; Laurin, M.; Gopinath, C. S.; Libuda, J.; Freund, H. J., On the Role of Different Adsorption and Reaction Sites on Supported Nanoparticles during a Catalytic Reaction: NO Decomposition on a Pd/Alumina Model Catalyst, *J. Phys. Chem. B* **2004**, 108, 14244-14254.
4. Ketteler, G.; Ogletree, F.; Bluhm, H.; Liu, H.; Eleonore, L. D.; Hebenstreit.; Salmeron, M. "In Situ Spectroscopic Study of the Oxidation and Reduction of Pd(111)" *J. Am. Chem. Soc.* **2005**, 127, 18269–18273.
5. Rose, M. K.; Borg, A.; Dunphy, J. C.; Mitsui, T.; Ogletree, D. F.; Salmeron, M. "Chemisorption of atomic oxygen on Pd(111) studied by STM" *Surf. Sci.* **2004**, 561, 69–78.
6. (a) Engel, T.; Ertl, G. "A molecular beam investigation of the catalytic oxidation of CO on Pd (111)" *J. Chem. Phys.* **1978**, 69, 1267–1281. (b) Engel, T. "A molecular beam investigation of He, CO and O_2 scattering from Pd(111)" *J. Chem. Phys.* **1978**, 69, 373–384. (c) Engel, T.; Ertl, G. "Elementary Steps in the Catalytic Oxidation of Carbon Monoxide on Platinum Metals" *Adv .Catal.* **1979**, 28, 1–78.
7. (a) Zaera, F.; Gopinath, C. S. "On the mechanism for the reduction of nitrogen monoxide on Rh(111) single-crystal surfaces" *Phys. Chem. Chem. Phys.,* **2003**, 5, 646–654. (b) Zaera, F.; Gopinath, C. S. "Evidence for an N_2O intermediate in the catalytic reduction of NO to N_2 on rhodium surfaces" *Chem. Phys. Lett.* **2000**, 332, 209–214. (c) Gopinath, C. S.; Zaera, F., NO + CO + O_2 reaction kinetics

on Rh(111): A molecular beam study, *J. Catal.* **2001**, 200, 270–287. (d) Bustos, V.; Gopinath, C. S.; Uñac, R.; Zaera, F.; Zgrablich, G. "Lattice-gas study of the kinetics of catalytic conversion of NO–CO mixtures on rhodium surfaces" *J. Chem. Phys.* **2001**, 114, 10927–10931.(e) Peden, C. H. F., Goodman, D. W., Blair, D. S., Berlowitz, P. J., Fisher, G. B., and Oh, S. H., "Kinetics of carbon monoxide oxidation by oxygen or nitric oxide on rhodium(111) and rhodium(100) single crystals" *J. Phys. Chem.* **1988**, 92, 1563-1567. (f) Permana H,; Ng, K. Y. S.; Peden, C. H. F.; Schmieg, S. J.; Lambert, D. K.; Belton, D. N., "Adsorbed species and reaction rates for NO-CO-O_2 over Rh(111)", *Catal. Lett.* **1997**, 47, 5–15. (g) Zaera, F.; Gopinath, C. S. "Role of adsorbed nitrogen in the catalytic reduction of NO on rhodium surfaces" *J. Chem. Phys.* **1999**, 111, 8088–8097.

8. Thirunavukkarasu, K.; Gopinath, C. S. "Fabrication of an Effusive Molecular Beam Instrument for Surface Reaction Kinetics — CO Oxidation and NO Reduction on Pd(111) Surfaces" *Catal. Lett,* **2007**, 119, 50–58.
9. (a) Gopinath, C. S.; Thirunavukkarasu, K.; Nagarajan, S. "Kinetic Evidence for the Influence of Subsurface Oxygen on Palladium Surfaces Towards CO Oxidation at High Temperatures" *Chem. Asia J.* **2009**, 4, 74–80 (b) Nagarajan, S.; Thirunavukkarasu.; K.; Gopinath, C. S. "A Revisit to Carbon Monoxide Oxidation on Pd(111) Surfaces" *J. Phys Chem. C.* **2009,** 113, 7385–7397. (c) Thirunavukkarasu, K.; Nagarajan, S.; Gopinath, C. S. "Electronic decoupling of surface layers from bulk and its influence in oxidation catalysis: A molecular beam study" *Appl. Surf. Sci.* **2009**, 256, 443–448. (d) Nagarajan, S.; Thirunavukkarasu.; K.; Gopinath, C. S. Jonathan Counsell, J.; Gilbert, L.; Bowker, M. "Nitric Oxide Reduction with Ethanol on Palladium Surfaces: A Molecular Beam Study" *J. Phys. Chem. C* **2009,** 113, 9814–9819.
10. Titkov, A. I.; Salanov, A. N.; Segrey, V.; Boronin, K.; A. I. "TDS and XPS Study of Oxygen Diffusion into Subsurface layers of Pd(110)" *React. Kinet. Catal. Lett.* **2005**, 86, 371–379.
11. (a) Han, J.; Zemlyanov, D. Y.; Ribeiro, F. H. "Interaction of O_2 with Pd single crystals in the range 1–150 Torr: Surface morphology transformations" *Surf. Sci.* **2006**, 600, 2730–2744, (b) Han, J.; Zemlyanov, D. Y.; Ribeiro, F. H. "Interaction of O_2 with Pd single crystals in the range 1–150 Torr: Oxygen dissolution and reaction" *Surf. Sci.* **2006**, 600, 2752–2761.
12. (a) Kl ötzer, B.; Hayek, K.; Konvicka, C.; Lundgren, E.; Varga, P. "Oxygen-included surface phase transformation of Pd(111): sticking, adsorption, and desorption kinetics" *Surf. Sci.* **2001**, 482, 237–242. (b) Gabasch, H.; Unterberger, W.; Hayek, K.; Kl ötzer, B.; Kresse, G.; Klein, C.; Schmid, M.; Varga, P. "Growth and decay of the Pd(111)–Pd_5O_4 surface oxide: Pressure-dependent kinetics and structural aspects" *Surf. Sci.* **2006**, 600, 205–218.
13. Leisenberger,; F, P.; Koller, G.; Sock, M.; Surnev, S.; Ramsey, M. G.; Netzer, F. P.; Kl ötzer, B.; Hayek, K. "Surface and subsurface oxygen on Pd(111)" *Surf. Sci.* **2000**, 445, 380–393.
14. Kan, H. H.; Shumbera, R. B.; Weaver, J. F. "Adsorption and abstraction of oxygen atoms on Pd(111): Characterization of the precursor to PdO formation" *Surf. Sci.* **2008**, 602, 1337–1346.
15. (a) Wickam, D. T.; Banse, B. A.; Koel, B. "Adsorption of nitrogen dioxide and nitric oxide on Pd(111)" *Surf. Sci.* **1991**, 243, 83–95. (b) Banse, B.A.; Koel, B.E. "Interaction of oxygen with Pd(111): High effective O_2 pressure conditions by using nitrogen dioxide" *Surf. Sci.* **1990**, 232, 275.
16. Sandler, Y. L.; Durigon, D. D. "The Low-Temperature Isotopic Oxygen Equilibration on Oxidized Palladium" *Journal of Physical Chemistry,* **1969**, 73, 2392–2396.
17. Hoffman, A.; Guo, X. C.; Yates, J.T. Jr. "Adsorption kinetics and isotopic equilibration of oxygen adsorbed on the Pd(111) surface" *J. Chem. Phys.* **1989**, 90, 5787.
18. (a) Thirunavukkarasu, K.; Thirumoorthy, K.; Libuda, J.; Gopinath, C. S. "Isothermal Kinetic Study of Nitric Oxide Adsorption and Decomposition on Pd(111) Surfaces: Molecular Beam Experiments" *J. Phys. Chem. B* **2005**, 109, 13283–13290. (b) Thirunavukkarasu, K.; Thirumoorthy, K.; Libuda, J.; Gopinath, C. S. "A Molecular Beam Study of the NO + CO Reaction on Pd(111) Surfaces" *J. Phys. Chem. B* **2005**, 109, 13272–13282. (c) Gopinath, C. S.; Zaera, F., "Transient kinetics during the isothermal reduction of NO by CO on Rh(111) as studied with effusive collimated molecular beams", *J. Phys. Chem. B* **2000**, 104, 3194-3203.
19. Ladas, S.; Imbhil, R.; Ertl, G. "Kinetic Oscillation During The Catalytic CO Oxidation on Pd(110) The Role of Subsurface Oxygen" *Surf. Sci.* **1989**, 219, 88–106.
20. (a) Conrad, H.; Ertl, G.; Kuppers, J.; Latta, E. E. "Interaction of NO and O_2 with Pd(111) surfaces I " *Surf. Sci,* **1977**, 65, 235-244.(b) Conrad, H.; Ertl, G.; Kuppers, J.; Latta, E. E. "Interaction of NO and O_2 with Pd(111) surfaces II " *Surf. Sci,* **1977**, 65, 245–260.
21. Su, S. C.; Carstens, J. N.; Bell, A. T. "A Study of the Dynamics of Pd Oxidation and PdO Reduction by H_2 and CH_4" *J. Catal.,* **1998,** 176 **,** 125–135.
22. Bondzie, V. A.; Kleban, P.H.; Dwyer, D.J. "Kinetics of PdO formation and CO reduction on Pd(110)" *Surf. Sci.* **2000**, 465, 266–276.
23. Voogt, E. H.; Mens, A. J. M.; Gijzeman, O. L. J.; Geus, J. W. "Adsorption of oxygen and surface oxide formation on Pd(111) and Pd foil studied with ellipsometry, LEED, AES and XPS" *Surf. Sci.* **1997**, 373, 210–220.
24. (a) Zheng, G.; Altman, E. I. "The oxidation of Pd(111)" *Surf. Sci.* **2000**, 462, 151–168. (b) Zheng, G.; Altman, E. I. "The oxidation mechanism of Pd(100)" *Surf. Sci.* **2002**, 504, 253–270. (c) Zheng, G.; Altmann, E. I. "The Reactivity of Surface Oxygen Phases on Pd(100) Toward Reduction by CO" *J. Phys. Chem. B* **2002**, 106, 1048–1057.
25. (a) Lundgren, E.; Kresse, G.; Klein, C.; Borg, M.; Andersen, J. N.; Santis, M. D.; Gauthier, Y.; Konvicka, C.; Schmid, M.; Varga, P. **"**Two-Dimensional Oxide on Pd(111)" *Phys. Rev. Lett.* 88 (2002) 246103–1. (b) Westerström, R.; Weststrate, C. J.; Gustafson, J.; Mikkelsen, A.; Schnadt, J.; Andersen, J. N.; Lundgren, E.; Seriani, N.; Mittendorfer, F.; Kresse, G. "Lack of surface oxide layers and facile bulk oxide formation on Pd(110)" *Phys. Rev. B*, **2009**, 80, 125431.
26. M. Todorova, E. Lundgren, V. Blum, A. Mikkelsen, S. Gray, J. Gustafson, M. Borg, J. Rogal, K. Reuter, J.N. Andersen, M. Scheffler, "The Pd(100)–($\sqrt{5}\times\sqrt{5}$) R27°-O surface oxide revisited" *Surf. Sci.* 2003, 541, 101-112.
27. Salo, P.; Honkala, K.; Alatalo, M.; Laasonen, K. "Catalytic oxidation of CO on Pd(111)" *Surf. Sci.* **2002**, 516, 247–253
28. (a) Lundgren, E.; Gustafson, J.; Mikkelsen, A.; Andersen, J. N.; Stierle, A.; Dosch, H.; Todorova, M.; Rogal, J.; Reuter, K.; Scheffler, M. "Kinetic Hindrance during the Initial Oxidation of Pd(100) at Ambient Pressures" *Phys. Rev. Lett.* **2004**, 92, 046101. (b) Todorova, M.; Reuter, K.; Scheffler, M. "Oxygen Overlayers on Pd(111) Studied by Density Functional Theory" *J. Phys. Chem. B* **2004**, 108, 14477–14483.
29. Markovits, A.; Minot. C. "On the move of strongly chemisorbed species on metals: The example of O diffusion on Pd(111) surface" *Chem. Phys. Lett.,* **2008**, 458, 92–95.
30. (a) Zemlyanov, D.; Kiss, B. A.; Kleimenov, E.; Teschner, D.; Zafeiratos, S.; Hävecker, M.; Knop-Gericke, A.; Schlogl, R.; Gabasch, H.; Unterberger, W.; Hayek, K.; Klotzer, B. "In situ XPS study of Pd(1 1 1) oxidation. Part 1: 2D oxide formation in 10^{-3} mbar O_2" *Surf. Sci.* **2006**, 600, 983–994. (b) Teschner, D.; Pestryakov, A.; Kleimenov, E.; Haevecker, M.; Bluhm, H.; Sauer, H.; Knop-Gericke, A.; Schlogl, R. "High-pressure X-ray photoelectron spectroscopy of palladium model hydrogenation catalysts. Part 1: Effect of gas ambient and temperature" *J. Catal.* **2005**, 230, 186–194.
31. Bondzie, V. A.; Kleban, P.; Dwyer, D. J. "XPS identification of the chemical state of subsurface oxygen in the O/Pd(110) system" *Surf. Sci.* **1996**, 347, 319–328.

32. Gabasch, H.; Hayek, K.; Kl ötzer, B.; Unterberger, W.; Kleimenov, E.; Teschner, D.; Zafeiratos, S.; Hävecker, M. Gericke, A. K.; Schlögl, R.; Kiss, B. A.; Zemlyanov, D "Methane Oxidation on Pd(111): In Situ XPS Identification of Active Phase" *J. Phys. Chem. C,* **2007**, 111, 7957–7962.
33. Gabasch, H.; Unterberger, W.; Hayek, K.; Klötzer, B.; Kleimenov, E.; Teschner, D.; Zafeiratos, S.; Haevecker, M.; Gericke, A. K.; Schlögl, R.; Han, J.; Ribeiro, F. H.; Kiss, B. A.; Curtin, T.; Zemlyanov, D " *In situ* XPS study of Pd(111) oxidation at elevated pressure, Part 2: Palladium oxidation in the 10^{-1} mbar range" *Surf. Sci*. **2006**, 600, 2980-2989.
34. K.S. Kim, A.F. Gossmann, N. Winograd, "X-ray photoelectron spectroscopic studies of palladium oxides and the palladium-oxygen electrode" *Anal. Chem.* **1974**, 46, 197-200.
35. (a) Weissman, D.L.; Shek, M. L.; Stefan, P. M.; Spicer, W. E. "Photoemission Spectra and Thermal Desorption Characteristics of Two States of Oxygen on Pd" *Surf, Sci.* **1980**, 92, L59–L66. (b) Weissman, D.L.; Shek, M. L.; Stefan, P. M.; Lindau, I.; Spicer, W. E. "The temperature dependence of the interaction of oxygen with Pd(111); A study by photoemission and auger spectroscopy" *Surf. Sci.* **1983,** 127, 513–525.
36. Corro, G.; Vāzquez-Cuchillo, O.; Banuelos, F.; Fierro, J. L.G.; Azomoza, M. "An XPS evidence of the effect of the electronic state of Pd on CH_4 oxidation on Pd/γ–Al_2O_3 catalysts" *Catalysis Communications,* **2007**, 8, 1977–1980.
37. Nakai, I.; Kondoh, H.; Shimada, T.; Resta, A.; Andersen, J. N.; Ohta, T. "Mechanism of CO oxidation reaction on O-covered Pd(111)surfaces studied with fast x-ray photoelectron spectroscopy: Change of reaction path accompanying phase transition of O domains" *J. Chem. Phys.* **2006**, 124, 224712–8.
38. Hicks, R.F.; Qi. H.; Young, M.L.; Lee, R. G. "Effect of Catalyst Structure on Methane Oxidation over Palladium on Alumina" *J. Catal.,* **1990**, 122, 295–306.
39. Farrauto, R. J.; Hobson, M. C.; Kennelly, T.; Waterman, E. M. "Catalytic chemistry of supported palladium for combustion of methane" *Appl. Catal. A: Gen.*, **1992**, 81, 227–237.
40. (a) Lyubovsky, M.; Pfefferle, L. "Methane combustion over the α-alumina supported Pd catalyst: Activity of the mixed Pd/PdO state" *Appl. Catal. A: Gen.* **1998**, 173, 107–119. (b) Lyubovsky, M.; Pfefferle, L. "Complete methane oxidation over Pd catalyst supported on a-alumina. Influence of temperature and oxygen pressure on the catalyst activity" *Catal. Today,* **1999**, 47, 29–44
41. Rebholz, M.; Matolin, V.; Prim, R.; Kruse, N. "Methanol decomposition on oxygen precovered and atomically clean Pd(111) single crystal surfaces" *Surf. sci.* **1991,** 251/252, 1117–1122.
42. Burch, R.; Urbano, F. J. "Investigation of the active state of supported palladium catalysts in the combustion of methane" *Appl. Catal. A: General* **1995**, 124, 121–138.
43. (a) Roy, S.; Hegde, M. S.; Ravishankar, N.; Madras, G. "Creation of Redox Adsorption Sites by Pd^{2+} Ion Substitution in nanoTiO_2 for High Photocatalytic Activity of CO Oxidation, NO Reduction, and NO Decomposition" *J. Phys. Chem. C* **2007,** 111, 8153–8160. (b) Roy, S.; Marimuthu, A.; Hegde, M. S.; Madras, G. "High rates of CO and hydrocarbon oxidation and NO reduction by CO over $Ti_{0.99}Pd_{0.01}O_{1.99}$" *Appl. Cata B: Environmental,* **2007**, 73, 300–310.
44. Baidya, T.; Gupta, A.; Deshpandey, P. A.; Madras, G.; Hegde, M. S. "High Oxygen Storage Capacity and High Rates of CO Oxidation and NO Reduction Catalytic Properties of $Ce_{1-x}Sn_xO_2$ and $Ce_{0.78}Sn_{0.2}Pd_{0.02}O_{2-\delta}$" *J. Phys. Chem. C* **2009,** 113, 4059–4068.
45. Schalow, T.; Brandt, B.; Starr, D. E.; Laurin, M.; Shaikhutdinov, S. K.; Schauermann, S.; Libuda, J.; Freund, H-J "Size-Dependent Oxidation Mechanism of Supported Pd Nanoparticles" *Angew. Chem. Int. Ed.* **2006**, 45, 3693 –3697.
46. Golunski, S. E.; York, A. P. E. "The Taylor Conference 2009" *Platinum Metals Rev.*, **2009**, 53, 221–225.
47. Somorjai, G. *Introduction to Surface Chemistry and Catalysis*; Wiley-Interscience: New York, 1994; p 363
48. (a) Bowker, M.; Morgan, C.; Perkins, N.; Holroyd, R.; Fourre, E.; Grillo, F.; MacDowall A.; "Ethene Adsorption, Dehydrogenation and Reaction with Pd(110): Pd as a Carbon 'Sponge"' *J. Phys. Chem. B,* **2005**, 109, 2377-2386. (b) Bowker, M.; Holroyd, R.; Perkins, N.; Bhantoo, J.; Counsell, J.; Carley, A.; Morgan, C. "Acetaldehyde adsorption and catalytic decomposition on Pd(110) and the dissolution of carbon" *Surface Science*, **2007**, 601, 3651–3660. (c) Bowker, M.; Counsell, J.; El-Abiary, K.; Gilbert, L.; Morgan, C.; Nagarajan, S.; Gopinath, C. S., "Carbon dissolution and segregation in Pd(110)" *J. Phys. Chem. C* **2010,** 114, 5060–5067.
49. (a) Gabasch, H.; Kleimenov, E.; Teschner, D., Zafeiratos, S.; Hävecker, M.; Gericke, A. K.; Schlögl, R.; Zemlyanov, D.; Kiss, B. A.; Hayek, K.; Klötzer, B, "Carbon incorporation during ethene oxidation on Pd(111) studied by in situ X-ray photoelectron spectroscopy at 2 $\times 10^{-3}$ mbar" *Journal of Catalysis* **2006**, 242, 340–348.(b) Gabasch, H.; Gericke, A. K.; Schlögl, Unterberger, W.; R.; Hayek, K.; Klötzer, B, "Ethene Oxidation on Pd(111): Kinetic Hysteresis Induced by Carbon Dissolution" *Catal. Lett.* **2007,** 119, 191–198.
50. Han, Y.-F.; Kumar, D.; Sivadinarayana, C.; Clearfield, A.; Goodman, D. W. "The formation of PdC_x over Pd-based catalysts in vapor-phase vinyl acetate synthesis: does a Pd–Au alloy catalyst resist carbide formation?" *Catal. Lett.* **2004**, 94, 131–134.
51. Teschner, D.; Borsodi, J.; Wootsch, A.; Révay, Z.; Hävecker, M.; Knop-Gericke, A.; David Jackson, S.; Schlögl, R. "The Roles of Subsurface Carbon and Hydrogen in Palladium-Catalyzed Alkyne Hydrogenation" *Science* **2008**, 320, 86–89.

Sankaranarayanan Nagarajan is currently a PhD student in the Catalysis Division, National Chemical Laboratory, Pune. He received B.Sc. Chemistry (2004) and M.Sc. Chemistry (2006) from The American College, Madurai. His research interest involves Surface Science, and Heterogeneous Catalysis on Single Crystal Surfaces. He visited Cardiff University, UK as a part of bilateral collaboration work with Prof. Michael Bowker for two months between June and August 2009. He participated and gave an oral presentation in Taylor conference, Cardiff University. He has published 5 research papers.

Chinnakonda S. Gopinath did PhD in electronic structure of ceramic superconductors from Indian Institute of Technology, Madras on 1993. Subsequently, he was awarded Alexander von Humboldt Fellowship and worked at Forschungszentrum Karlsruhe. Then he moved to work at University of California, Riverside on nitric oxide reduction with a molecular beam instrument (MBI). He returned to India to take up Scientist position at National Chemical Laboratory (NCL), Pune on 2000. Independently he designed and fabricated MBI at NCL and initiated surface science studies at NCL, Pune. His field of specialization is surface science and heterogeneous catalysis. Apart from the above, he has been working on making new materials, including visible light driven photocatalysts and mesoporous materials, bridging the material and pressure gap problem in catalysis, and fundamental aspects of environmental catalysis. Recently he has been invited to be a CNRS Professor at UCCS, Lille. He has authored more than 100 publications, and recipient of bronze medal of CRSI, India.